Interface and Molecular Electronic Structure vs Tunneling Characteristics of CH₃- and CF₃-Terminated Thiol Monolayers on Au(111)

Qiang Sun and Annabella Selloni*

Chemistry Department, Princeton University, Princeton, New Jersey 08540

Received: July 31, 2006; In Final Form: September 3, 2006

By means of density functional theory calculations, we investigate work functions, energy level alignments, charge transfers, and tunneling characteristics of CH₃- and CF₃-terminated alkane- and diphenylthiol monolayers on Au(111). While the alignments of the energy levels and the charge transfers at the metal−molecule interface are found to be determined by the value of the clean Au surface work function relative to the HOMO ionization potential (IP) at the thiolate end of the monolayer, the change of work function for the modified Au(111) surface is dominated by the properties of the thiolate monolayer, including the character, saturated or conjugated, of the molecule and the chemical nature and orientation of the terminal group. The tunneling currents through the adsorbed molecular monolayers are calculated using the Tersoff−Hamann approach. The computed difference between the $I-V$ characteristics for the CH₃- and CF₃-terminated alkanethiol monolayers agree well with available experimental data. The energy barrier at the metal−molecule interface, the molecular electronic structure, and the IP of the terminal group are the key parameters which determine the tunneling properties.

1. Introduction

There is currently considerable interest in using self-assembled monolayers (SAMs) of dipolar organic molecules to tailor the effective work functions of metal and semiconductor surfaces and to control the energetic barriers for charge injection.[1−22] There is experimental evidence that the work function can be tuned by using molecules with different characteristics, e.g., different terminal functional groups,[2,3,5,7,13,19,21] while the atomic scale contact between the molecule and the metal determines the alignment of the frontier orbitals of the molecule with respect to the metal Fermi energy E_F.[4,10,11,14,23−25] In particular, the energy separation ΔE between E_F and the closest molecular level (typically the highest occupied molecular orbital, HOMO) is one of the main parameters governing the overall characteristics of molecular devices.[10,22,25] Recent theoretical studies have addressed the origin of the work function changes and interface barriers induced by the adsorbed monolayers, and detailed analyses have been reported for a few representative cases.[26,27] However, a number of interesting issues have not been theoretically addressed yet, e.g., the differences in interfacial electrostatics between monolayers of saturated and conjugated molecules of similar length and termination, or between monolayers of aliphatic molecules of different lengths and terminations. Most important, no theoretical study is available on the correlation between the interface electrostatics and the electron tunneling characteristics of the molecular monolayers, which are among the properties of greatest practical and fundamental interest for these systems.

In this work, we try to bridge this gap by a parallel study of the interface electronic properties and the $I-V$ tunneling characteristics—as measured, e.g., by scanning tunneling microscopy (STM) or conductive-probe atomic force microscopy (CP-AFM)—of prototype SAMs of thiol molecules on the Au-(111) surface.[20,28,29] We theoretically investigate how the interface barrier, ΔE, and the effective work function, Φ, depend on the molecular properties, by considering conjugated (dibenzenethiol) and saturated (alkanethiol) molecules with different terminal groups (X = CH₃, CF₃) as model compounds. Unlike CH₃, the CF₃ terminal group has an intrinsic dipole; thus, the molecular dipoles of the CF₃-terminated alkanethiols show an even−odd dependence on the number of methylene groups in the chain.[19,30] We evaluate the $I-V$ curves through the molecular monolayer within the simple Tersoff−Hamann approach and elucidate their relation to the interface and molecular electronic structures.

2. Computational Details

The calculations have been performed within the plane wave−pseudopotential approach using density functional theory (DFT) in the generalized gradient approximation.[31] Details of the method and the parameters used in the present work, such as kinetic energy cutoff for the plane wave basis set as well as the pseudopotentials, have been reported previously.[32] A repeated slab geometry was used to model the Au(111) surfaces, with a separation d_z of ∼33 Å between successive Au(111) slabs, and the theoretical lattice constant obtained in ref 32. We used a surface ($\sqrt{3} \times \sqrt{3}$) $R30°$ unit cell with one adsorbed dibenzenethiolate (SPh₂X, with X = CH₃, CF₃) or alkanethiolate (SC_nH_{2n}X, with n = 4, 5, 7 and X = CH₃, CF₃) every three surface Au atoms, corresponding to full monolayer coverage (see Figure 1). The molecules in the gap between two slabs are adsorbed through a S−Au bond on one Au(111) surface, while a vacuum gap of at least 21 Å separates the apex of the molecule from the bottom surface of the next slab (see Figure 1). In this
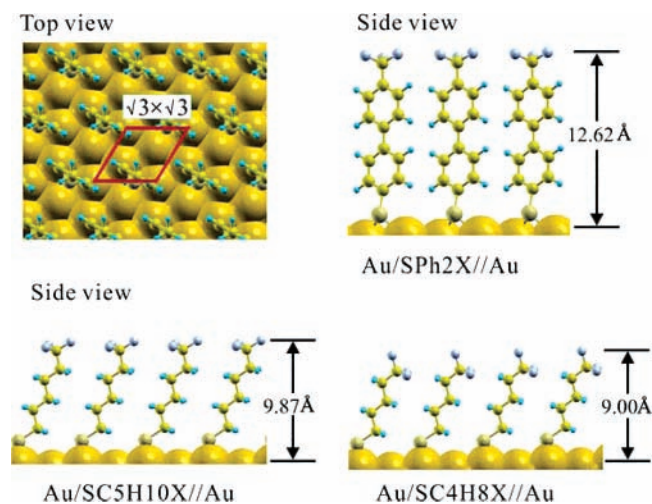
Figure 1. Computed geometries for the investigated conjugated and saturated molecular monolayers with different terminal groups (X = CH₃, CF₃) on Au(111).

way, we make sure to eliminate all interaction between the molecular terminal and the next Au surface. The Brillouin zone was sampled with 48 special k-points for the $(\sqrt{3} \times \sqrt{3})$ $R30°$ cell. In the geometry optimizations, all coordinates were relaxed until each component of the residual force on each atom was smaller than 0.03 eV/Å.

3. Results and Discussion

Despite extensive research over many years,[33] the headgroup structure for adsorbed thiolates on Au(111) is not fully established yet. Different adsorption sites for the S headgroup have been proposed, e.g., recent photoelectron diffraction experiments have found evidence for adsorption at top sites,[34] while the bridge−fcc site is the most stable one according to state-of-the-art DFT calculations.[35−37] In this work, we restrict our consideration to the theoretically optimized structures. For all investigated molecules, the sulfur headgroup is at the bridge− fcc site, and the S−Au bond lengths are ∼2.49 Å. For the alkanethiolate monolayers, our calculations yield a tilt angle of about 23°, against an experimental value of about 30°.[33] For the SPh₂X monolayers, the optimized geometry at full coverage shows practically no tilt of the molecular axis.

For each adsorbed monolayer, the work function Φ has been calculated from the energy difference between the value of the electrostatic potential in the vacuum region and the Fermi energy E_F (see Figure 2). The dipole layer arising in the vacuum gap region because of the periodic boundary conditions was subtracted. The position ΔE of the molecular HOMO (which is mostly derived from the S p orbitals) relative to E_F was determined from the highest occupied peak in the projected density of states (PDOS) onto the S atom (see Figure 3). The resulting values of ΔE and $\Delta \Phi$ for the different monolayers are reported in Table 1, where $\Delta \Phi$ is the work function change with respect to clean Au(111). For the latter, our calculated value is 5.4 eV (experimental value: 5.31 eV[25]). In agreement with recent theoretical studies,[26,27] we find that ΔE has practically the same value, $\Delta E \approx -0.96$ eV, for all the investigated molecules, despite the large differences in their physical and chemical characteristics. By contrast, the value of $\Delta \Phi$ depends markedly on the terminal group: the work function increases ($\Delta \Phi > 0$) for the CF₃-terminated molecules, while it decreases ($\Delta \Phi < 0$) when the terminal group is CH₃ (Figure 2). Table 1 also shows small differences (a few tenths of an electronvolt)
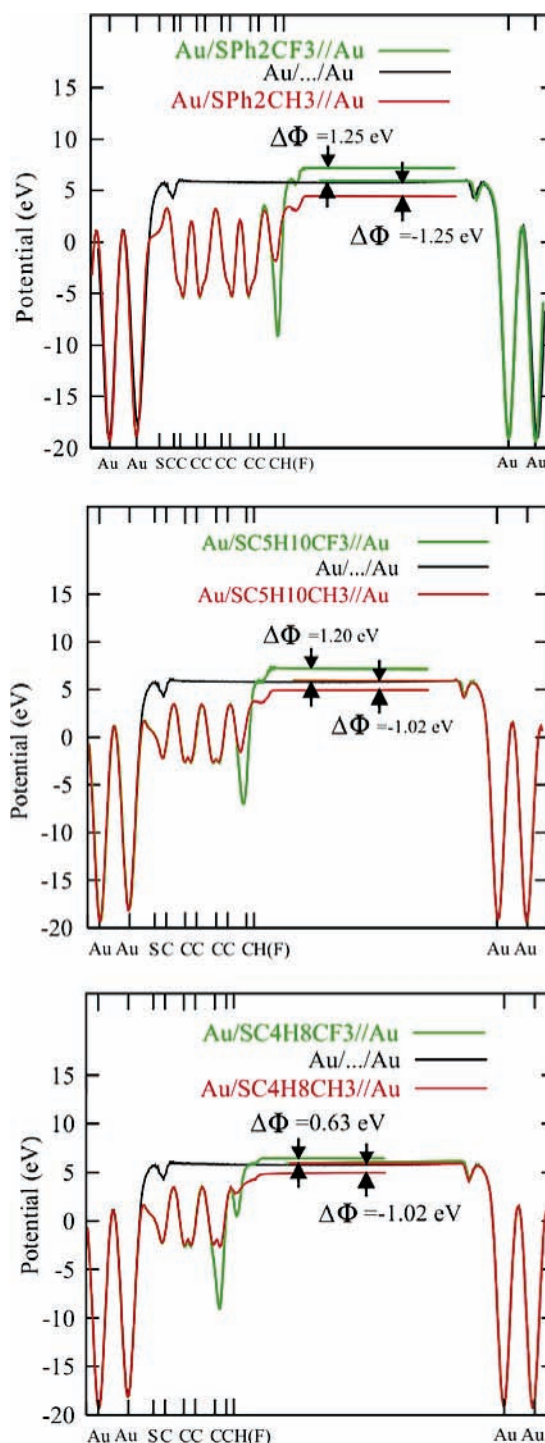
Figure 2. Plane-averaged electrostatic potential for the clean (black line) and modified Au(111) surfaces (red/green line: CH₃/CF₃-terminated molecular monolayers). The energy zero is set at the Fermi energy. To show the even−odd effect for the CF₃-terminated alkanethiol monolayers, results for both SC₅H₁₀X (X = CH₃, CF₃; middle panel) and SC₄H₈X (bottom panel) are presented.

between the work functions of conjugated and saturated monolayers. Moreover, for saturated molecules with CF₃ termination, an even−odd effect with respect to the number of methylene units in the molecular chain is present.

To provide a rationale for these results, we consider the isolated monolayers of SPh₂X and SC$_n$H$_{2n}$X molecules (radicals) in the same geometries they have when they are adsorbed on the Au(111) surface. Following ref 26, we notice that for a two-dimensional layer of dipolar molecules the space can be divided
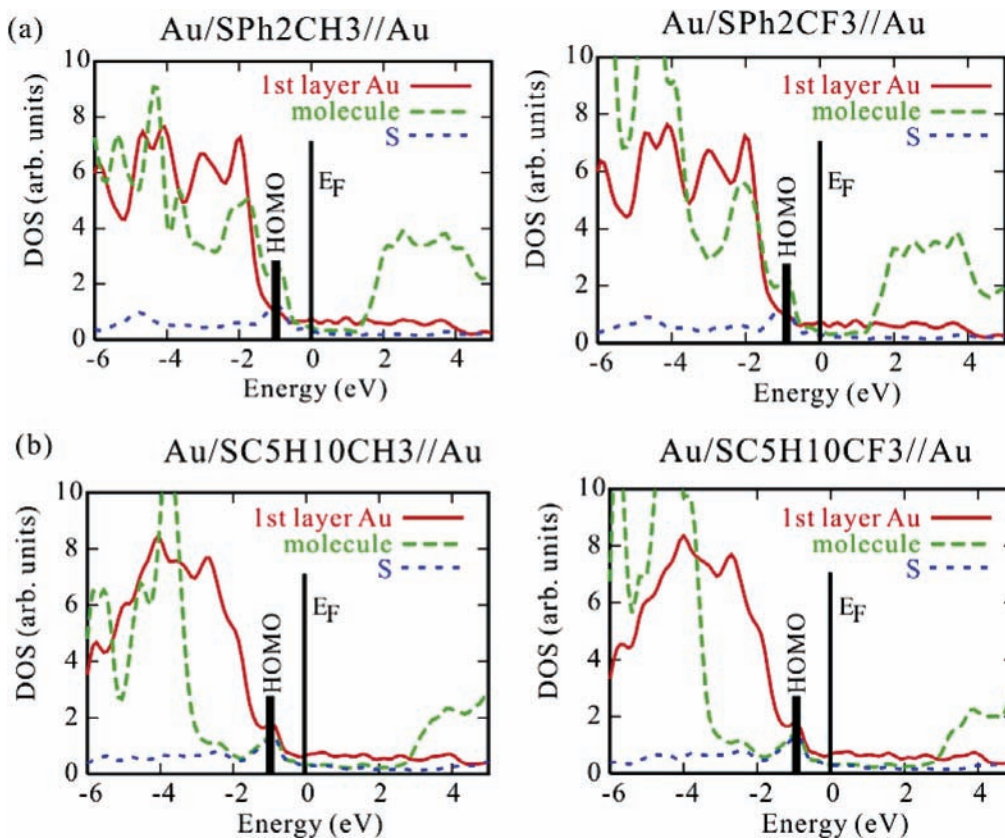
Figure 3. Projected density of states for different adsorbed molecular monolayers on Au(111). The dashed green (blue) line is the PDOS for the whole adsorbed molecule (the S headgroup only).

TABLE 1[a]

	ΔE (eV)	$\Delta\Phi$	$IP_{monolayer}^{left}(S)$	$IP_{monolayer}^{right}(S)$	ΔV_{vac}	$IP_{sam}^{right}(S)$	$\Delta IP^{right}(X)$
SPh_2CH_3	−0.96	−1.25	7.2	4.15	−3.05	5.1	0.0
$HSPh_2CH_3$			6.2	5.35	−0.85		
$SC_4H_8CH_3$	−0.96	−1.02	7.2	5.4	−1.8	5.3	0.2
$SC_5H_{10}CH_3$	−0.96	−1.02	7.2	5.4	−1.8	5.3	0.2
$SC_7H_{14}CH_3$	−0.96	−1.02	7.2	5.4	−1.8	5.3	0.1
SPh_2CF_3	−0.96	1.25	7.2	7.2	0.0	7.6	0.0
$SC_4H_8CF_3$	−0.96	0.63	7.2	7.5	0.3	7.0	0.2
$SC_5H_{10}CF_3$	−0.96	1.20	7.2	8.3	1.1	7.6	0.1
$SC_7H_{14}CF_3$	−0.96	1.20	7.2	8.3	1.1	7.6	0.1

[a] HOMO energy relative to the Fermi energy, ΔE; work function modification, $\Delta\Phi$ (see Figure 2), with respect to the calculated workfunction, $\Phi = 5.4$ eV, for clean Au(111); left and right ionization potentials, $IP_{monolayer}^{left}$ and $IP_{monolayer}^{right}$, of the isolated monolayer of neutral SPh_2X or $SC_nH_{2n}X$ radicals (X = CH_3, CF_3); step in the vacuum level across the isolated monolayers, ΔV_{vac}; ionization potential of the adsorbed SAM, IP_{sam}^{right}; change of ionization potential of the terminal group upon adsorption, $\Delta IP^{right}(X)$. All values are in eV.

into two regions, one adjacent to the S headgroup (hereafter called "left") and the other next to the terminal group (called "right"), with different vacuum levels, V_{vac}^{left} and V_{vac}^{right} (determined from the plane-averaged electrostatic potential along the direction perpendicular to the two-dimensional layer), so that the step in the electrostatic potential across the molecular layer can be expressed as $\Delta V_{vac} = V_{vac}^{right} - V_{vac}^{left}$. Consequently, the ionization potential (IP) of the molecular monolayer now depends on which side an electron in a certain molecular level (typically the HOMO) escapes. We shall thus distinguish a left (side of the S headgroup) and a right (side of the X terminal) ionization potential, $IP_{monolayer}^{left}(S)$ and $IP_{monolayer}^{right}(S)$, where S between parentheses indicates that the orbital (HOMO) from which the electron is extracted is centered on the S atom. These ionization potentials are calculated from the energy difference between the energy of the HOMO and the V_{vac}^{left} and V_{vac}^{right} vacuum levels, respectively. For the different molecular monolayers with different terminal groups, the $IP_{monolayer}^{left}(S)$ values

are identical (see Table 1). In contrast, the $IP_{monolayer}^{right}(S)$ values strongly depend on the terminal group X as well as on the fact that the molecule is conjugated or saturated. Since the level alignment ΔE is determined by the difference between the clean surface work function and $IP_{monolayer}^{left}(S)$, it is clearly the same for the various molecules, as found also in refs 26 and 27.

With respect to the HOMOs ($IP_{monolayer}^{left}(S)$) of the isolated neutral SPh_2X and $SC_nH_{2n}X$ monolayers, the HOMOs of the adsorbed layers appear to be shifted upward by more than 1.0 eV. (Notice, however, that the HOMOs of the adsorbed layers are practically unshifted when compared to the HOMOs of the isolated monolayers of the H-saturated $HSPh_2X$ and $HSC_nH_{2n}X$ molecules; see Table 1 and ref 26). This indicates that some charge is transferred from the metal surface to the sulfur headgroup upon adsorption. A significant charge redistribution and the formation of dipoles at the interface is evident in plots of the difference charge density (not shown).
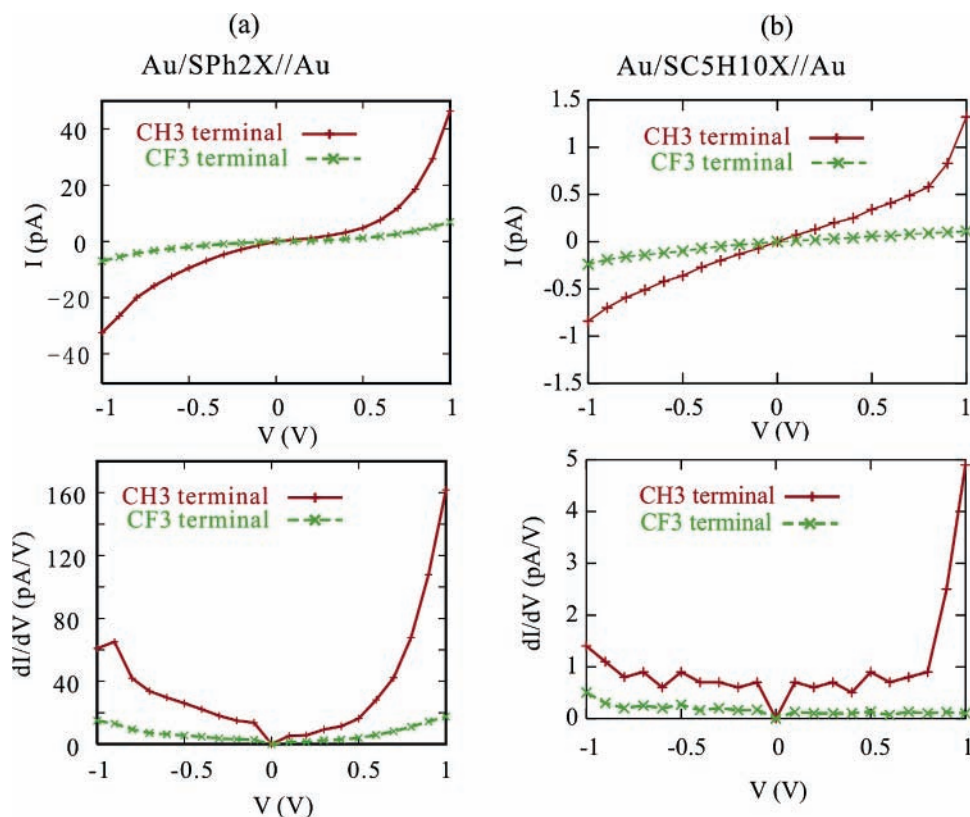
Figure 4. Calculated tunneling current per molecule as a function of the applied bias for conjugated (a) and saturated (b) molecular monolayers with CH_3 and CF_3 terminal groups. Lower panels show the corresponding dI/dV curves, obtained by numerically differentiating the $I-V$ curves in the upper panels.

We have also determined the change of IP for the terminal groups upon adsorption, $\Delta IP^{right}(X)$, by considering the position of the highest occupied level in the PDOS for the molecular terminal before and after adsorption of the molecular monolayer. As shown in Table 1, for the conjugated molecular layers $\Delta IP^{right}(X)$ is zero, meaning that the IP of the terminal group is not affected by the interface dipole. This can be attributed to the screening by the delocalized electrons in the conjugated molecules. For the saturated molecular monolayers, instead, $IP^{right}(X)$ decreases by about $0.1-0.2$ eV, as the screening of the interfacial dipole is in this case incomplete.

An additional interesting aspect of the results in Table 1 is the even−odd effect for the CF_3-terminated alkanethiol monolayers (see also Figure 2), as the $IP^{right}_{monolayer}(S)$ for $SC_5H_{10}CF_3$ is about 0.8 eV larger than that for $SC_4H_8CF_3$. From the geometries of the two adsorbed molecules (Figure 1), we can see that for $SC_5H_{10}CF_3$ the (local) dipole of the CF_3 terminal is directed along the surface normal, while for $SC_4H_8CF_3$, there is an angle of ∼50° with respect to the surface normal. Thus, the work function and IP of the former molecule (even number of C atoms) is larger than that of the latter one (odd number of carbons), as found also experimentally.[19,30]

The current−voltage ($I-V$) characteristics of adsorbed molecular monolayers are most frequently measured by STM or by CP-AFM. With reference to this kind of experimental setup, we have performed calculations of the $I-V$ curves based on a simple extension of Tersoff−Hamann's (TH's) theory of the STM.[38] The use of this approximate theory can be generally justified under the condition that the tunneling probability for a valence electron located on the topmost group of atoms to return to the metal is larger than that of tunneling through the vacuum gap, a situation that is typically found in relatively short molecules (for an interesting discussion of the applicability of

TH's theory, see ref 39). Here, an additional reason for using this simplified approach is that we are mostly interested in comparing the currents through monolayers which have all the same barrier ΔE at the metal−molecule interface. Extending TH's theory to finite (but still small with respect to the system work function) voltages V, we express the tunneling current per molecule as

$$I \approx e v_{eff} \int_A dxdy \int_{E_F}^{E_F + eV} dE \rho_s(x, y, z_0 : E) \qquad (1)$$

where $\rho_s(x, E)$ is the local density of states (LDOS) of the Au(111)/SAM system at zero applied bias, A is the surface area per molecule, z_0 is the vertical position of the STM tip, and v_{eff} is an effective velocity of the tunneling electrons. For z_0, we take a point in the vacuum gap ∼2.0 Å above the apex of the molecule, where the tails of the charge density of the successive slab are negligible. To estimate v_{eff} in eq 1, we tested two different possibilities, either taking v_{eff} equal to the Fermi velocity for gold or deriving it from the decay constant of $\rho_s(\mathbf{r}, E_F)$ in the vacuum, and found very similar results.

The computed $I-V$ curves for SPh_2X and $SC_5H_{10}X$ (X = $-CH_3$, $-CF_3$) are reported in Figure 4. From these curves, we numerically calculated the conductance dI/dV, which are shown in the lower part of Figure 4. As the applied voltage must be small with respect to Φ, we restrict V to the range $-1 \leq V \leq 1$ V. First of all, we remark that the computed current for the conjugated monolayers is more than a factor of 10 larger than for the alkanethiols. Within the logic of Tersoff−Hamann's approach, this is attributed to the larger LDOS around E_F at the terminal of the conjugated molecules, as indeed suggested by Figure 3 (see also Figures 3a and 6 of ref 40, comparing the LDOS at E_F and the PDOS, respectively, of $PhCH_3$- and C_4H_8-

11400 *J. Phys. Chem. A, Vol. 110, No. 40, 2006*

Letters

CH$_3$-terminated molecules similar to those of interest in this work). Second, by comparing molecules with the same backbone but different terminal groups, we can see that the tunneling current for the CH$_3$ terminal is larger than that for CF$_3$, in nice agreement with recent measurements for decanethiol monolayes on gold.[29] Again, this difference between the two different terminations is due to the larger PDOS in proximity of E_F for the CH$_3$ terminal (which can be clearly seen in Figure 4b of ref 40). It may also be interesting to note that, since the current within Tersoff−Hamanns's approach is determined by the LDOS in the vacuum region above the molecular apex, our calculations are not expected to show any significant dependence on the sulfur adsorption site.

In conclusion, using DFT calculations, we have studied how the interface electronic structure affects the $I−V$ tunneling characteristics of monolayers of conjugated and saturated organic molecules on Au(111). While the energy alignment and charge transfer at the metal−molecular monolayer interface are solely determined by the work function of the clean metal surface and the molecular ionization potential at the thiolate end of the monolayer, the change of work function appears to be dominated by the molecular properties. The $I−V$ characteristics, calculated within the Tersoff−Hamann approach, illustrate the strong dependence of the tunneling current on molecular properties for SAMs with the same chemical bond to the gold surface. The good qualitative agreement between the computed $I−V$ curves and the experiment further suggests that the most important tunneling barrier for the investigated systems is through the vacuum region between the molecule and the tip.

References and Notes

(1) Ulman, A. *Chem. Rev.* **1996**, *96*, 1533.

(2) Evans, S. D.; Ulman, A. *Chem. Phys. Lett.* **1990**, *170*, 462.

(3) Campbell, I. H.; Rubin, S.; Zawodzinski, T. A.; Kress, J. D.; Martin, R. L.; Smith, D. L.; Barashkov, N. N.; Ferraris, J. P. *Phys. Rev. B* **1996**, *54*, R14321.

(4) Campbell, I. H.; Kress, J. D.; Martin, R. L.; Smith, D. L.; Barashkov, N. N.; Ferraris, J. P. *Appl. Phys. Lett.* **1997**, *71*, 3528.

(5) Zehner, R. W.; Parsons, B. F.; Hsung, R. P.; Sita, L. R. *Langmuir* **1999**, *15*, 1121.

(6) Bruening, M.; Cohen, R.; Guillemoles, J. F.; Moav, T.; Libman, J.; Shanzer, A.; Cahen, D. *J. Am. Chem. Soc.* **1997**, *119*, 5720.

(7) Bastide, S.; Butruille, R.; Cahen, D.; Dutta, A.; Libman, J.; Shanzer, A.; Sun, L.; Vilan, A. *J. Phys. Chem. B* **1997**, *101*, 2678.

(8) Lu, J.; Delamarche, E.; Eng, L.; Bennewitz, R.; Meyer, E.; Guntherodt, H. J. *Langmuir* **1999**, *15*, 8184.

(9) Vilan, A.; Shanzer, A.; Cahen, D. *Nature (London)* **2000**, *404*, 166.

(10) Ratner, M. A. *Nature (London)* **2000**, *404*, 137.

(11) Ashkenasy, G.; Cahen, D.; Cohen, R.; Shanzer, A.; Vilan, A. *Acc. Chem. Res.* **2002**, *35*, 121.

(12) Beebe, J. M.; Engelkes, V. B.; Miller, L. L.; Frisbie, C. D. *J. Am. Chem. Soc.* **2002**, *124*, 11268.

(13) Bruner, E. L.; Koch, N.; Span, A. R.; Bernasek, S. L.; Kahn, A.; Schwartz, J. *J. Am. Chem. Soc.* **2002**, *124*, 3192.

(14) Chabinyc, M. L.; Chen, X.; Holmlin, R. E.; Jacobs, H.; Skulason, H.; Frisbie, C. D.; Mujica, V.; Ratner, M. A.; Rampi, M. A.; Whitesides, G. M. *J. Am. Chem. Soc.* **2002**, *124*, 11730.

(15) Crispin, X.; Geskin, V.; Crispin, A.; Cornil, J.; Lazzaroni, R.; Salaneck, W. R.; Bredas, J. L. *J. Am. Chem.* Soc. **2002**, *124*, 8131.

(16) Howell, S.; Kuila, D.; Kasibhatla, B.; Kubiak, C. P.; Janes, D.; Reifenberger, R. *Langmuir* **2002**, *18*, 5120.

(17) Selzer, Y.; Salomon, A.; Cahen, D. *J. Am. Chem. Soc.* **2002**, *124*, 2886.

(18) Vondrak, T.; Wang, H.; Winget, P.; Cramer, C. J.; Zhu, X. Y. *J. Am. Chem. Soc.* **2000**, *122*, 4700.

(19) Alloway, D. M.; Hofmann, M.; Smith, D. L.; Gruhn, N. E.; Graham, A. L.; Colorado, R.; Wysocki, V. H.; Lee, T. R.; Lee, P. A.; Armstrong, N. R. *J. Phys. Chem. B* **2003**, *107*, 11690.

(20) Engelkes, V. B.; Beebe, J. M.; Frisbie, C. D. *J. Am. Chem. Soc.* **2004**, *126*, 14287.

(21) de Boer, B.; Hadipour, A.; Mandoc, M. M.; van Woudenbergh, T.; Blom, P. W. M. *Adv. Mater.* **2005**, *17*, 621.

(22) Kim, B. S.; Beebe, J. M.; Jun, Y.; Zhu, X. Y.; Frisbie, C. D. *J. Am. Chem. Soc.* **2006**, *128*, 4970.

(23) Nesher, G.; Vilan, A.; Cohen, H.; Cahen, D.; Amy, F.; Chan, C.; Hwang, J.; Kahn, A. *J. Phys. Chem. B* **2006**, *110*, 14363.

(24) Selzer, Y.; Salomon, A.; Cahen, D. *J. Phys. Chem. B* **2002**, *106*, 10432.

(25) Xue, Y.; Datta, S.; Ratner, M. A. *J. Chem. Phys.* **2001**, *115*, 4292.

(26) Heimel, G.; Romaner, L.; Bredas, J. L.; Zojer, E. *Phys. Rev. Lett.* **2006**, *96*.

(27) Rousseau, R.; DeRenzi, V.; Mazzarello, R.; Marchetto, D.; Biagi, R.; Scandolo, S.; delPennino, U. *J. Phys. Chem. B* **2006**, *110*, 10862.

(28) Wold, D. J.; Frisbie, C. D. *J. Am. Chem. Soc.* **2001**, *123*, 5549.

(29) Pflaum, J.; Bracco, G.; Schreiber, F.; Colorado, R.; Shmakova, O. E.; Lee, T. R.; Scoles, G.; Kahn, A. *Surf. Sci.* **2002**, *498*, 89.

(30) Graupe, M.; Takenaga, M.; Koini, T.; Colorado, R., Jr.; Lee, T. R. *J. Am. Chem. Soc.* **1999**, *121*, 3222.

(31) Perdew, J. P.; Burke, K.; Ernzerhof, M. *Phys. Rev. Lett.* **1996**, *77*, 3865.

(32) Piccinin, S.; Selloni, A.; Scandolo, S.; Car, R.; Scoles, G. *J. Chem. Phys.* **2003**, *119*, 6729.

(33) Schreiber, F. *Prog. Surf. Sci.* **2000**, *65*, 151.

(34) Kondoh, H.; Iwasaki, M.; Shimada, T.; Amemiya, K.; Yokoyama, T.; Ohta, T.; Shimomura, M.; Kono, S. *Phys. Rev. Lett.* **2003**, *90*, 066102.

(35) Hayashi, T.; Morikawa, Y.; Nozoye, H. *J. Chem. Phys.* **2001**, *114*, 7615.

(36) Vargas, M. C.; Giannozzi, P.; Selloni, A.; Scoles, G. *J. Phys. Chem. B* **2001**, *105*, 9509.

(37) Gottschalck, J.; Hammer, B. *J. Chem. Phys.* **2002**, *116*, 784.

(38) Tersoff, J.; Hamann, D. R. *Phys. Rev. B* **1985**, *31*, 805.

(39) Eigler, D. M.; Weiss, P. S.; Schweizer, E. K.; Lang, N. D. *Phys. Rev. Lett.* **1991**, *66*, 1189.

(40) Sun, Q.; Selloni, A.; Scoles, G. *J. Phys. Chem. B* **2006**, *110*, 3493.